Journal of Bioenergetics and Biomembranes, Vol. 37, No. 4, August 2005 (© 2005)
DOI: 10.1007/s10863-005-6635-z

Intracellular Ca^{2+} Pools and Fluxes in Cardiac Muscle-Derived H9c2 Cells

Antonio Lax,[1] Fernando Soler,[1] and Francisco Fernández-Belda[1,2]

Received March 30, 2005; accepted May 9, 2005

Relevant Ca^{2+} pools and fluxes in H9c2 cells have been studied using fluorescent indicators and Ca^{2+}-mobilizing agents. Vasopressin produced a cytoplasmic Ca^{2+} peak with half-maximal effective concentration of 6 nM, whereas thapsigargin-induced Ca^{2+} increase showed half-maximal effect at 3 nM. Depolarization of the mitochondrial inner membrane by protonophore was also associated with an increase in cytoplasmic Ca^{2+}. Ionomycin induced a small and sustained depolarization, while thapsigargin had a small but transient effect. The thapsigargin-sensitive Ca^{2+} pool was also sensitive to ionomycin, whereas the protonophore-sensitive Ca^{2+} pool was not. The vasopressin-induced cytoplasmic Ca^{2+} signal, which caused a reversible discharge of the sarco-endoplasmic reticulum Ca^{2+} pool, was sensed as a mitochondrial Ca^{2+} peak but was unaffected by the permeability transition pore inhibitor cyclosporin A. The mitochondrial Ca^{2+} peak was affected by cyclosporin A when the Ca^{2+} signal was induced by irreversible discharge of the intracellular Ca^{2+} pool, i.e., adding thapsigargin. These observations indicate that the mitochondria interpret the cytoplasmic Ca^{2+} signals generated in the reticular store.

KEY WORDS: Ca^{2+} pools; thapsigargin; vasopressin; sarco-endoplasmic reticulum; cytoplasmic Ca^{2+}; mitochondrial Ca^{2+}; cardiomyocyte.

INTRODUCTION

The ability of Ca^{2+} to act as ubiquitous intracellular messenger depends on the coordinated action of many different transporters and regulatory molecules (Berridge *et al*., 2003; Clapham, 1995). Early studies measuring spatially averaged Ca^{2+} levels revealed that some increases in cytoplasmic Ca^{2+} were transient showing variable amplitude and duration (Allen and Blinks, 1978; Yue *et al*., 1986), whereas others displayed an oscillatory pattern (Woods *et al*., 1986). Indeed, the regular pulses of Ca^{2+} that drive each heartbeat is a good example of Ca^{2+}-induced oscillatory phenomenon (Berridge, 2003).

The advance in Ca^{2+} imaging techniques for measuring the dynamics of intracellular Ca^{2+} (Rudolf *et al*., 2003) has confirmed that the final functional outcome conveyed by a Ca^{2+} signal is encoded not only by the amplitude but also by the spatial and temporal profile. The current view is that the wide range of Ca^{2+} signals are assembled from a Ca^{2+} signaling toolkit based on specific interactions between local signals and target molecules (Bootman *et al*., 2001).

A cytoplasmic Ca^{2+} increase, which acts as an intracellular signal, is the result of Ca^{2+} exit from intracellular pools and/or Ca^{2+} entry from the extracellular space. The sarco-endoplasmic reticulum (SER) is the main intracellular Ca^{2+} store, and the Ca^{2+} stored within this organelle is essential for protein folding and maturation. Likewise, the exit of Ca^{2+} from SER serves as a trigger for cardiac muscle contraction (Berridge, 2002). Furthermore, during

[1] Departamento de Bioquímica y Biología Molecular A, Facultad de Veterinaria, Universidad de Murcia, Murcia, Spain.
[2] To whom correspondence should be addressed; e-mail: fbelda@um.es.

Abbreviations used: SER, sarco-endoplasmic reticulum; EGTA, ethylene glycol-bis(β-aminoethyl ether)-*N*,*N*,*N*′,*N*′-tetraacetic acid; Hepes, 4-(2-hydroxyethyl)piperazine-1-ethanesulfonic acid; IP_3, inositol 1,4,5-trisphosphate; VP, [Arg^8]-vasopressin; TG, thapsigargin; BHQ, 2,5-di(*t*-butyl)-hydroxybenzene; CCCP, carbonyl cyanide *m*-chlorophenylhydrazone; TMRM, tetramethylrhodamine methyl ester; ECM, extracellular medium; IO, ionomycin; $\Delta\Psi_m$, mitochondrial inner membrane potential; CsA, cyclosporin A.

the last decade mitochondrial Ca^{2+} has gained a relevant role in cellular signaling (Duchen, 2000) and other intracellular Ca^{2+} pools, such as the Golgi apparatus, have also been described (Missiaen *et al*., 2001; Pinton *et al*., 1998).

The complex Ca^{2+} signal is well suited for regulating multiple physiological processes, while the failure of such a control activates a number of self-destructive events including organelle dysfunction, cytoskeletal structure derangement, chromatin fragmentation, and other effects leading to apoptotic cellular death (Orrenius *et al*., 2002).

There is little doubt that alteration of intracellular Ca^{2+} homeostasis is associated with several heart diseases, including ischemic injury. In this respect, the clonal H9c2 cells constitute a well accepted model for investigating cardiac ischemia *in vitro* (He *et al*., 1999; Mestril *et al*., 1994; Mizukami *et al*., 2000; Tanno *et al*., 2003) because they possess many of the functional mechanisms found in adult cardiac myocytes. In our study, we have measured cytoplasmic and mitochondrial Ca^{2+} responses as well as the relationship between Ca^{2+} and $\Delta\Psi_m$ when different Ca^{2+}-mobilizing agents were used. The experiments were performed with the aid of suitable fluorescence probes and were directed at characterizing the intracellular Ca^{2+} pools and fluxes in H9c2 cells that might be relevant for Ca^{2+} signaling.

MATERIALS AND METHODS

Materials

The H9c2 cell line derived from rat heart embryonic myocytes was obtained from the European Collection of Cell Cultures (www.ecacc.org.uk) at passage 34 and maintained through passage 44. The culture was grown at 37°C in a humidified atmosphere containing 5% CO_2. Cells plated on 150-mm tissue culture dishes were subcultured or harvested when they reached ~70% confluence. For confocal microscopy examination, cells were seeded on 35-mm glass bottom dishes.

Reagents and Media

Acetoxymethyl derivatives of Fura-2, Rhod-2, and Fluo-3, as well as Pluronic® F-127 and TMRM, were from Molecular Probes Europe (www.probes.com). VP, TG, BHQ, CCCP, IO from *Streptomyces conglobatus*, CsA, and all other reagents of analytical grade were supplied by Sigma. $CaCl_2$, in the form of Titrisol® standard solution, was purchased from Merck. Dulbecco's modified Eagle's medium containing low glucose and L-glutamine, fetal bovine serum, penicillin-streptomycin-L-glutamine solution, and other culture reagents were obtained from Gibco.

The culture medium was Dulbecco's modified Eagle's medium supplemented with 10% fetal bovine serum, 2 mM L-glutamine, 100 units/mL penicillin, and 100 μg/mL streptomycin. The trypsinization medium containing 0.25% trypsin was from Gibco. ECM with Ca^{2+} had the following composition: 10 mM Hepes, pH 7.4, 121 mM NaCl, 1 mM $CaCl_2$, 1.2 mM $MgSO_4$, 5 mM $NaHCO_3$, 1.2 mM KH_2PO_4, 10 mM glucose, and 0.25% bovine serum albumin. The pH was readjusted when 0.2 mM sulfinpyrazone was added to the medium. ECM with EGTA, i.e., in the absence of Ca^{2+}, was prepared by substituting 1 mM $CaCl_2$ by 2.2 mM EGTA. The loading medium was ECM with Ca^{2+} supplemented with 2 μM Ca^{2+} indicator, 0.02% Pluronic® F-127 and 0.2 mM sulfinpyrazone. Stock aliquots of Rhod-2 ester form were freshly reduced to the corresponding nonfluorescent dihydroRhod-2 derivative by adding solid sodium borohydride (Bowser *et al*., 1998) before dilution with ECM. DihydroRhod-2 was selectively oxidized inside the mitochondria giving specificity to the evaluation of the mitochondrial Ca^{2+}. TMRM loading and measurements were performed in the absence of sulfinpyrazone.

Dependence on Free Ca^{2+}

Free Ca^{2+} was adjusted by varying the concentration ratio of $CaCl_2$/EGTA as described by Fabiato (1988). The computer program for the calculations took into account the absolute stability constant for the Ca^{2+}-EGTA complex (Schwartzenbach *et al*., 1957), EGTA protonation equilibria (Blinks *et al*., 1982), the presence of Ca^{2+} ligands, and the pH value.

Loading of Fluorescent Indicators

Plated cells were incubated at 37°C for 30 min with loading medium containing the Ca^{2+} indicator ester form (2 μM). For microscopic observation, cells loaded with Fluo-3 or dihydroRhod-2 were washed twice and reincubated for 30 min in ECM with Ca^{2+}. Cells loaded with Fura-2 or dihydroRhod-2, to be used in spectrofluorometric measurements, were detached from plates and then washed and resuspended at 2–4 $\times$ 10^6 cells/mL in ECM with Ca^{2+}. The cell suspension was maintained at 37°C for 30 min to allow the intracellular liberation of the indicator

free acid form. Cells were used for fluorescence measurements for up to 3 h after the loading/de-esterification periods. Alternatively, detached cells were incubated at 37°C for 15 min with ECM containing Ca^{2+} and supplemented with 0.2 μM TMRM. In all cases, cells were resuspended at 25°C in ECM with Ca^{2+} before measurements.

Confocal Imaging

Fluorescence was visualized with laser-scanning confocal equipment from Leica Microsystems consisting of a DM IRE II inverted fluorescence microscope coupled to a TCS SP2 scanhead module. Samples were observed through an HCX PL APO 63× oil immersion objective with numerical aperture 1.32. The confocal planes selected were those showing the largest nuclear diameters. Fluo-3 was excited by the argon-ion laser and the emission signal was collected through the 504–530 nm range. Excitation of Rhod-2 and TMRM was accomplished by the green helium-neon laser. Wavelength intervals of 574–611 or 570–643 nm were selected for measuring the Rhod-2 or TMRM fluorescence emission, respectively. The pinhole was set at 140 μm giving a 1.1 μm thickness of the z slice.

Fluorescence in Cells Suspension

The fluorescence signal was measured at 25°C under continuous stirring in an Aminco-Bowman Series 2 spectrofluorometer. The experimental protocol was initiated by diluting the dye-loaded cell suspension in the cuvette immediately prior to trace recording. This provided $\sim 2 \times 10^5$ cells/mL in Fura-2 experiments and $\sim 3 \times 10^5$ cells/mL in the Rhod-2 and TMRM experiments. The procedure using the Fura-2 indicator was valid when the dilution media were ECM with EGTA or ECM with Ca^{2+} plus 10 mM Ni^{2+}. When the experiments were performed in ECM with Ca^{2+}, without Ni^{2+}, the dye-loaded cells were sedimented at 480 × g for 10 min and then resuspended in ECM with Ca^{2+} before measurements. When the dilution medium was ECM with EGTA, the concentration of free Ca^{2+} after dilution was 2.5 nM, which can be considered Ca^{2+}-free conditions for our purposes. In all the Fura-2 spectrofluorometric measurements 0.2 mM sulfinpyrazone was present.

For Fura-2 experiments, samples were excited at 340 and 380 nm and the emitted light was selected at 510 nm. The excitation and emission wavelengths for Rhod-2 measurements were 550 and 580 nm, respectively. TMRM fluorescence was evaluated at 546 and 573 nm as excitation wavelengths, while 590 nm was the emission wavelength. Cytoplasmic free Ca^{2+} was calculated from background-corrected fluorescence ratios ($R = F_{340}/F_{380}$) using the equation, $[Ca^{2+}] = K_d[(R - R_{\min})/(R_{\max} - R)] \times Q$ (Grynkiewicz *et al*., 1985). $R_{\max}$ was obtained at the end of each experiment in the presence of 1 mM free Ca^{2+} and 0.2% Triton X-100; $R_{\min}$ was estimated by adding 40 mM EGTA under Ca^{2+} saturating conditions. Q was the ratio $F_{\min}/F_{\max}$ at 380 nm. The autofluorescence of samples was determined separately by measuring F_{340} and F_{380} of Fura-2 unloaded cells. Fluorescence arising from the external medium due to the passive release of Fura-2 was negligible when cells were diluted in the absence of Ca^{2+}, i.e., when ECM with EGTA was the dilution medium. The extracellular fluorescence due to the presence of Ca^{2+} was quenched when ECM with Ca^{2+} was supplemented with 10 mM $NiCl_2$. When the experiments were performed in ECM with Ca^{2+}, but Ni^{2+} was not present, the loaded cells were sedimented and then resuspended in new ECM with Ca^{2+} to eliminate Fura-2 from the external medium. The apparent dissociation constant for the Ca^{2+}-Fura-2 complex was evaluated under our experimental conditions. F_{340}/F_{380} was measured at different Ca^{2+} concentrations after equilibration of cells loaded with Fura-2 ($\sim 2 \times 10^5$ cells/mL) in ECM with EGTA and 0.2% Triton X-100. Different free Ca^{2+} concentrations were established as described above. The calculated dissociation constant was 240 nM. The distribution of Fura-2 between cytoplasm and intracellular compartments was determined by loading plated cells at 37°C with the Ca^{2+} probe for different time periods. Cytoplasmic Fura-2 was released by incubating $\sim 5 \times 10^5$ cells/mL in ECM with Ca^{2+} plus 50 μM digitonin at 37°C for 5 min. Under these conditions, more than 95% of the cells were stained with 0.1% Trypan blue. The supernatant was reserved and the pellet was resuspended in ECM with Ca^{2+}. The fluorescence ratio of both fractions was evaluated in the presence of 0.2% Triton X-100. Mitochondrial Ca^{2+} was expressed as arbitrary units, i.e., $\Delta F/F \times 100$ because calibration of the nonratiometric and compartmentalized Rhod-2 is difficult and imprecise (Hajnóczky *et al*., 1995; Monteith and Blaustein, 1999). TMRM fluorescence was expressed as ratio units (F_{573}/F_{546}) or by first-order rate constants (1-100k).

Data Presentation

The traces shown in the figures are representative of five or more experiments. The software for smoothing the experimental traces used the Savitsky–Golay algorithm. Plotted data points correspond to an average of at least

three independent measurements. Standard deviations of mean values (plus or minus) are given. Curve fitting and calculation of first-order rate constants was carried out with the Sigma-Plot Graph System (version 8.0) from Jandel Scientific.

RESULTS

Confocal microscopy in conjunction with fluorescent indicators have been used for studying intracellular Ca^{2+} signaling in different cell types (Cheng *et al*., 1993; Koizumi *et al*., 1999; Thomas *et al*., 2000). In the conditions used in the current study, i.e., loading at 37°C for 30 min with the cell-permeable Fluo-3 derivative, H9c2 cells exhibited low fluorescence when incubated in ECM with Ca^{2+} (Fig. 1(A)). However, the fluorescence was more intense and extended to the whole cell when the Ca^{2+} gradients were collapsed by the Ca^{2+} ionophore IO (Fig. 1(B)). Likewise, the mitochondrial Ca^{2+} pool revealed by the compartmentalized indicator Rhod-2 exhibited a bright punctate distribution and was practically absent in the nuclear region (Fig. 1(C)). A similar pattern of spotty fluorescence was observed when the cells were loaded with the $\Delta\Psi_m$ indicator TMRM (Fig. 1(D)).

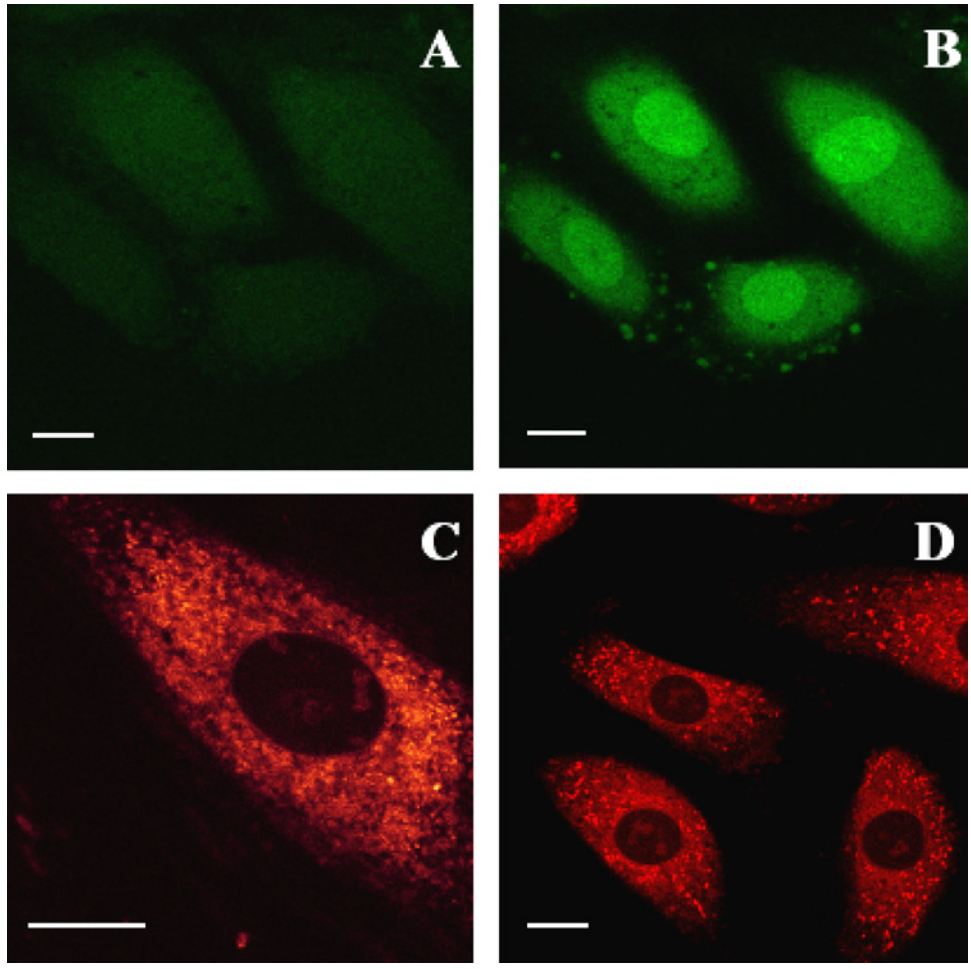

Fig. 1. Representative confocal images of H9c2 cells used in this study. Cells equilibrated in ECM with Ca^{2+} were loaded with Fluo-3 (A and B), dihydroRhod-2 (C), or TMRM (D). Nonstimulated cells maintain low fluorescence equally distributed within the cytoplasm and nucleus when loaded with Fluo-3 (A). The same field was visualized 5 s after addition of 5 μM IO (B). Ca^{2+} monitored with the probe Rhod-2 appears as punctate cytoplasmic fluorescence which is consistent with a mitochondrial location. (C) The maintenance of a $\Delta\Psi_m$ in living cells can be observed by the use of the mitochondrial indicator TMRM (D). Bars length is 50 μm. Fluorescence images show planes crossing the nuclei.

The next set of experiments on cytoplasmic Ca^{2+} was performed with the aid of the ratiometric indicator Fura-2. Initially, the distribution of Fura-2 in the cytoplasm and intracellular compartments was quantified after selective permeabilization of the plasma membrane. Our data indicate that over 80% of the Ca^{2+} probe was released by digitonin, i.e., was located in the cytoplasm.

Dose-response studies were carried out to determine the optimal concentration of Ca^{2+}-mobilizing agents and assess the contribution of relevant Ca^{2+} pools in our cell system. Ca^{2+} stored within the SER has been shown to be sensitive to physiological concentrations of the hormone VP (Chen and Chen, 1999; Szalai *et al.*, 2000; Thomas *et al.*, 1984). When H9c2 cells were resuspended in ECM with Ca^{2+} the resting cytoplasmic free Ca^{2+} was around 80 nM (Fig. 2(A)). Moreover, a typical cytoplasmic Ca^{2+} peak was apparent when cells preloaded with Fura-2 and resuspended in ECM with Ca^{2+} were challenged with 50 nM VP. When the experiment was extended to evaluate the effect of different VP concentrations, the threshold concentration was 0.3 nM and half-maximal activation was observed at 6 nM (Fig. 2(B)). The maximal VP effect transitorily increased the level of cytoplasmic Ca^{2+} ~6-fold. The sequential addition of ryanodine aliquots to the cell suspension did not cause any cytoplasmic Ca^{2+} response (data not shown).

The SER Ca^{2+} pool was also sensitive to the Ca^{2+}-ATPase inhibitor TG (Lytton *et al.*, 1991; Sagara and Inesi, 1991) and the addition of 3 μM TG to Fura-2 loaded cells provoked a cytoplasmic Ca^{2+} peak. When cells were resuspended in ECM with Ca^{2+} the transient rise was followed by an elevated steady state level (Fig. 3(A)). Nonetheless, when the measurements were performed in ECM with Ca^{2+} but supplemented with 10 mM Ni^{2+}, the transient rise of cytoplasmic Ca^{2+} returned to the initial resting level (Fig. 3(B)). When the experiments were performed in the absence or presence of 10 mM Ni^{2+}, subtraction of the Ca^{2+} values at each time point, showed a slow progressive increase in cytoplasmic Ca^{2+} to reach the above-mentioned elevated plateau phase (dotted trace in Fig. 3(B)).

When the cytoplasmic Ca^{2+} increase was measured using different TG concentrations and the dilution medium was ECM with Ca^{2+} plus 10 mM Ni^{2+}, the dose-response curve indicated that the threshold concentration was 0.2 nM (Fig. 4(A)). Moreover, the TG concentration producing half-maximal activation was 3 nM and the maximal effect increased the resting level of cytoplasmic Ca^{2+} ~2.5-fold. The SER Ca^{2+} pool was also sensitive to BHQ, another specific inhibitor of the intracellular Ca^{2+}-ATPase protein (Kass *et al.*, 1989). Measurements performed in ECM with Ca^{2+} plus 10 mM Ni^{2+} indicated that the threshold BHQ concentration was 100 nM and that the half-maximal effect was elicited by a concentration of 3 μM (Fig. 4(B)). The maximal BHQ effect increased the resting Ca^{2+} level ~2.5-fold.

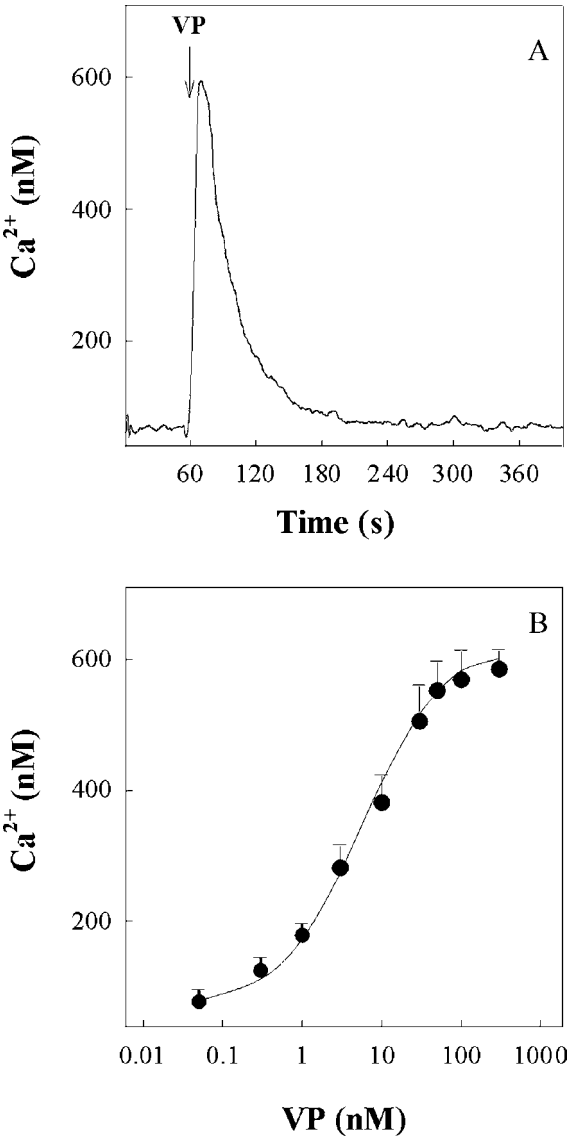

Fig. 2. Cytoplasmic Ca^{2+} response triggered by extracellular VP addition. Cells loaded with Fura-2 in ECM with Ca^{2+} were sedimented and resuspended in new ECM with Ca^{2+} before measurements. The final mixture composition was 10 mM Hepes, pH 7.4, 121 mM NaCl, 1 mM $CaCl_2$, 1.2 mM $MgSO_4$, 5 mM $NaHCO_3$, 1.2 mM KH_2PO_4, 10 mM glucose, 0.25% bovine serum albumin, 0.2 mM sulfinpyrazone, and ~ 2×10^5 cells/mL. The measurement temperature was 25°C. (A) Time-course of the Ca^{2+} signal when a 50 nM VP aliquot was added. (B) Dose-response dependence after addition of different VP concentrations. Ca^{2+} transients were measured at the peak value.

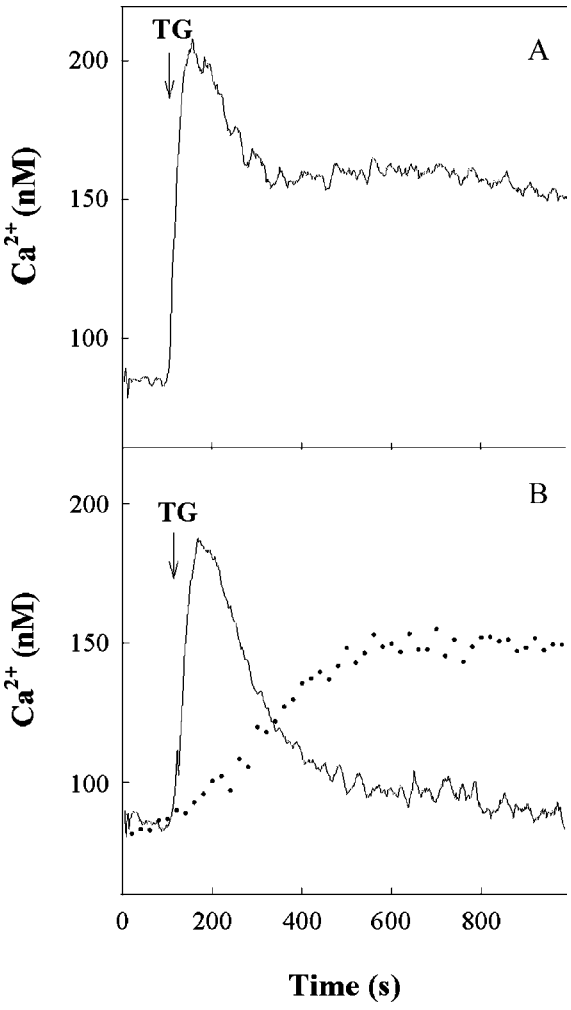

Fig. 3. Cytoplasmic Ca^{2+} response after addition of extracellular TG. ECM with Ca^{2+} was used for cells loading with Fura-2. The time-course of the fluorescence signal at 25°C was monitored under different assay conditions. (A) Loaded cells were resuspended in ECM with Ca^{2+}, giving a final mixture composition as described for Fig. 3. (B) Loaded cells were diluted 10-fold in ECM with Ca^{2+} but supplemented with 10 mM $NiCl_2$. Additions of 3 μM TG aliquots were made when indicated. Subtraction of the Ca^{2+} signal in both panels at each time point is shown as a dotted trace (panel B).

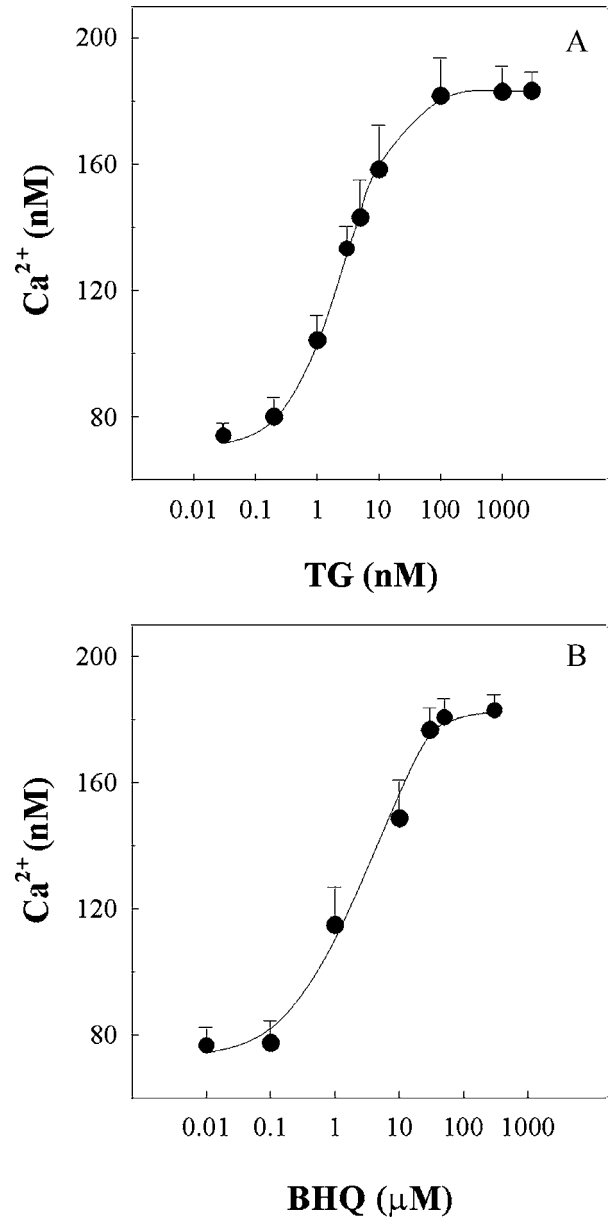

Fig. 4. Dose-response dependence after addition of agents discharging the SER Ca^{2+} pool. Cells loaded with Fura-2 were diluted 10-fold at the beginning of the experiments with ECM containing Ca^{2+} plus 10 mM Ni^{2+}. Sulfinpyrazone at 0.2 mM was present. Dependence of the cytoplasmic Ca^{2+} rise at 25°C was plotted as a function of the TG (A) or BHQ (B) concentrations used. Data points correspond to maximal fluorescence changes.

Ca^{2+} stored within the mitochondria can be released by the presence of the protonophore CCCP (Babcock *et al.*, 1997). Thus, the CCCP-induced release of mitochondrial Ca^{2+} was examined by measuring both the effect on cytoplasmic Ca^{2+} and $\Delta\Psi_m$. In these experiments, the preliminary dilution was performed with ECM containing Ca^{2+} plus 10 mM Ni^{2+}. The increase in cytoplasmic Ca^{2+} measured in Fura-2 loaded cells displayed a threshold concentration of 1 μM CCCP and a half-maximal effect at ~4 μM (Fig. 5(A)). The $\Delta\Psi_m$ was indirectly assessed with the aid of the fluorescent probe TMRM (Scaduto and Grotyohann, 1999). The fluorescence of TMRM-loaded cells decayed when CCCP was added to the incubation mixture. A family of curves was generated using different CCCP concentrations and the resulting first-order rate constants were evaluated. The dependence of the rate constants showed a sigmoidal

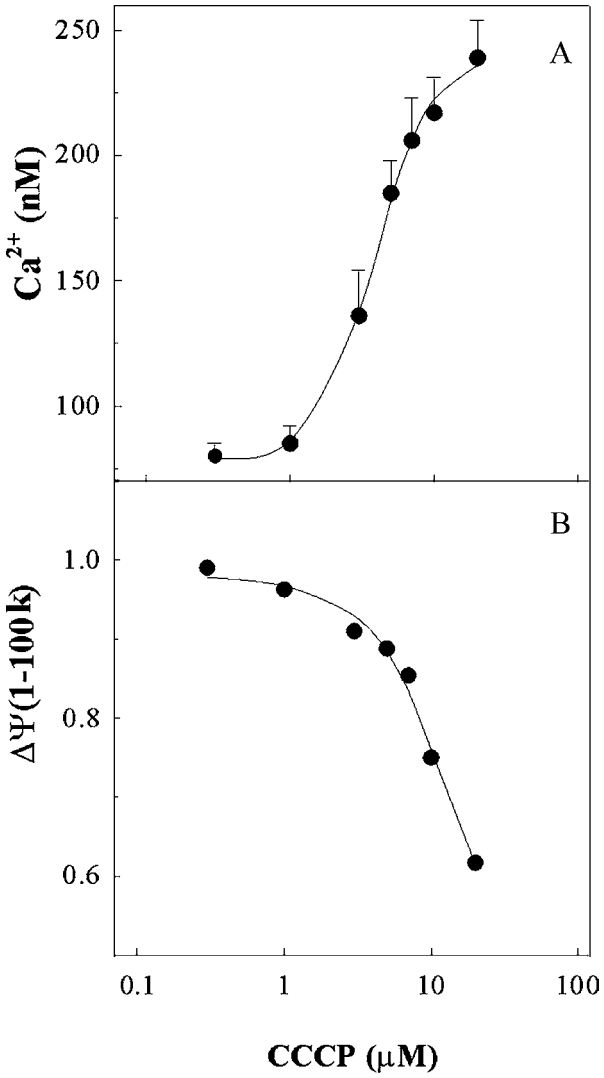

Fig. 5. The effect of CCCP on cytoplasmic Ca^{2+} and $\Delta\Psi_m$. (A) Cell loaded with Fura-2 in ECM with Ca^{2+} were diluted at $\sim 2 \times 10^5$ cells/mL using the same medium supplemented with 10 mM Ni^{2+} and 0.2 mM sulfinpyrazone. The cytoplasmic Ca^{2+} increase was evaluated after addition of different CCCP concentrations. (B) Cells loaded with TMRM were diluted to $\sim 3 \times 10^5$ cells/mL using ECM with Ca^{2+} plus 10 mM Ni^{2+}. First-order rate constants for fluorescence decrease were evaluated after addition of different CCCP concentrations. Apparent rate constants, expressed as 1-100k, are plotted against CCCP concentration. Measurements were carried out at 25°C.

increase when plotted against CCCP concentration on a logarithmic scale. Therefore, a plot of 1-*k vs.* CCCP displays a sigmoidal decay. Figure 5(B) shows a plot of 1-100*k* against CCCP on a logarithmic scale.

The time-dependent effect of Ca^{2+}-mobilizing agents on cytoplasmic Ca^{2+} was also tested using the same sample. Fura-2 loaded cells gave resting cytoplasmic free Ca^{2+} around 80 nM when diluted in ECM with Ca^{2+} plus 10 mM Ni^{2+}. The treatment of cells with 3 μM TG produced a transient increase in cytoplasmic Ca^{2+} and the subsequent addition of 5 μM CCCP was followed by another Ca^{2+} peak (Fig. 6, upper trace). When the dilution medium was ECM with EGTA, to establish Ca^{2+}-free conditions, the resting Ca^{2+} level was over 45 nM and the observed cytoplasmic Ca^{2+} response was qualitatively similar. Namely, cells successively treated with 3 μM TG and 5 μM CCCP, in the absence of external Ca^{2+}, caused transient increases in cytoplasmic Ca^{2+} although the amounts of Ca^{2+} released were smaller (Fig. 6, middle trace). The subsequent addition of 5 μM IO induced an additional release of Ca^{2+}. When the same stimulation protocol was applied but the order of the additions was changed, the observed effects were as follows: an excess of Ca^{2+} ionophore, i.e., 5 μM IO, released a large amount of Ca^{2+} when added first and the subsequent addition of TG had no further effect on cytoplasmic Ca^{2+} (Fig. 6, lower trace). However, a significant rise in cytoplasmic Ca^{2+} was still associated with the addition of CCCP.

The effect of different Ca^{2+}-mobilizing agents on $\Delta\Psi_m$ was tested in separate assays. The experiments were performed with TMRM-loaded cells and the dilution medium was ECM with Ca^{2+} to maintain the intracellular Ca^{2+} stores full. The addition of 5 μM CCCP was followed by a clear and time-dependent decrease in TMRM fluorescence (Fig. 7, upper trace). When the dilution medium was supplemented with 5 μM IO, a very fast but slight decrease in $\Delta\Psi_m$ was observed (middle trace). Furthermore, when 3 μM TG was added, $\Delta\Psi_m$ underwent a relatively slow and small decrease that was reversible (lower trace).

The existence of Ca^{2+} pools in SER and mitochondria, and the close contact between these organelles, has been shown to be functionally relevant under physiological conditions (Hajnóczky *et al.*, 2000; Szalai *et al.*, 2000). The relationship between relevant Ca^{2+} pools was analyzed by triggering a Ca^{2+} signal from SER and measuring the mitochondrial Ca^{2+} response. These experiments were performed using a dilution medium without Ca^{2+} to ensure that any triggering signal comes from intracellular sources. Thus, Rhod-2 loaded cells were diluted in ECM with EGTA to reach Ca^{2+}-free conditions in the external medium and the subsequent addition of 50 nM VP produced a Ca^{2+} peak inside the mitochondria (Fig. 8, upper trace). When the experiment was repeated with a preliminary 10 min incubation with 5 μM CsA before adding 50 nM VP, the transient increase in mitochondrial Ca^{2+} was still observed (Fig. 8, lower trace).

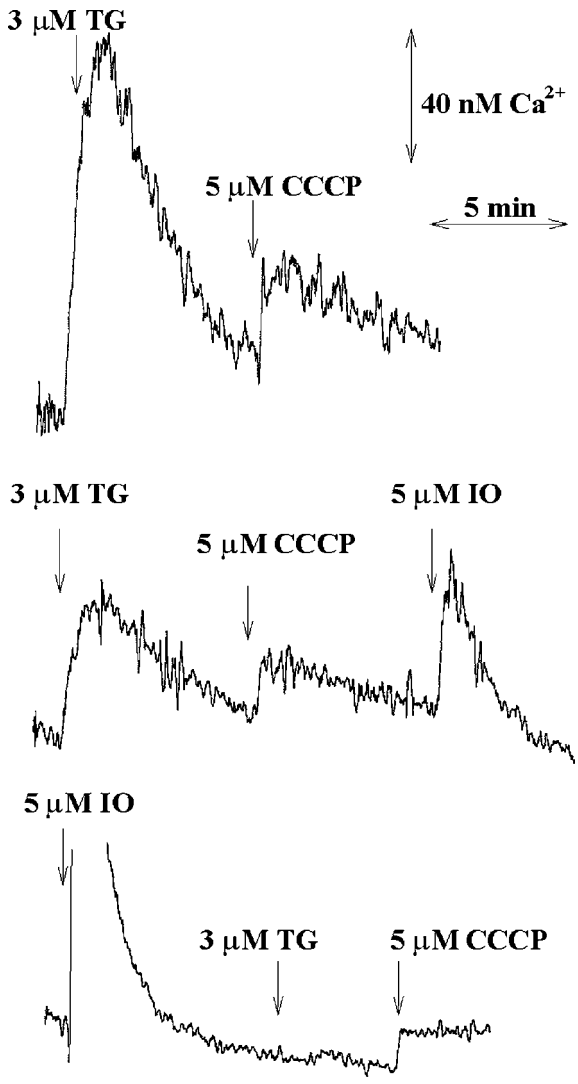

Fig. 6. Sensitivity of intracellular Ca^{2+} pools to different Ca^{2+}-mobilizing agents. A concentrated suspension of Fura-2 loaded cells in ECM with Ca^{2+} was diluted 10-fold at the beginning of the experiment (25°C). The dilution medium was ECM with Ca^{2+} plus 10 mM Ni^{2+} and the resting Ca^{2+} level was around 80 nM (*upper trace*). When the dilution medium was ECM with EGTA the resting free Ca^{2+} was around 45 nM (*middle and lower traces*). Sulfinpyrazone at 0.2 mM was present. TG, CCCP, and IO were added when indicated.

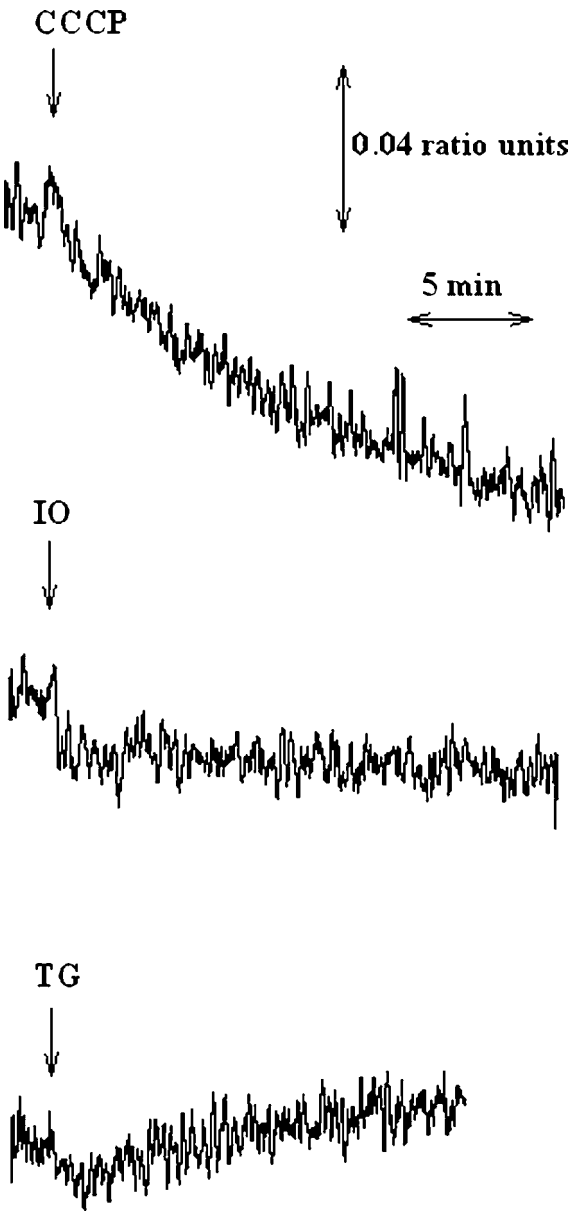

Fig. 7. Sensitivity of $\Delta\Psi_m$ to Ca^{2+}-mobilizing agents. Cells preloaded with TMRM in ECM containing Ca^{2+} were diluted at the beginning of the experiment with the same medium. The assay temperature was 25°C and the final mixture contained $\sim 3 \times 10^5$ cells/mL. The sensitivity to different agents: 5 μM CCCP, 5 μM IO, or 3 μM TG was tested in independent experiments.

The SER Ca^{2+} signal was also generated by a non-physiological mechanism, adding TG, and the mitochondrial response was measured in Rhod-2 loaded cells. The addition of 3 μM TG to cells previously diluted in ECM with EGTA was sensed by the mitochondria as a Ca^{2+} peak (Fig. 9, upper trace). However, when Rhod-2 loaded cells were preincubated for 10 min with 5 μM CsA, the extracellular addition of 3 μM TG was followed by a sustained increase in mitochondrial Ca^{2+} and not by an ebb and flow (Fig. 9, lower trace). In other words, the exit of Ca^{2+} from the mitochondria was prevented when CsA was added first to block the permeability transition pore (Altschuld *et al.*, 1992; Broekemeier *et al.*, 1989).

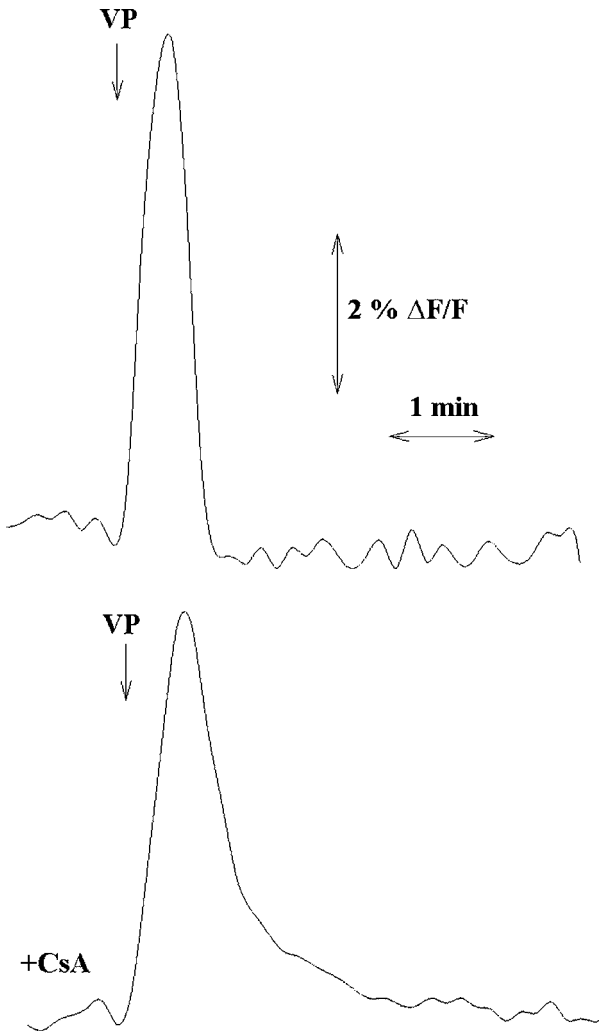

Fig. 8. Response of mitochondrial Ca^{2+} when the SER pool was stimulated with VP. Rhod-2 loaded cells in ECM with Ca^{2+} were diluted at 25°C with ECM containing EGTA to give ~3 $\times 10^5$ cells/mL in a nominally Ca^{2+}-free medium. Time-dependent response when 50 nM extracellular VP was added (*upper trace*). The VP addition was preceded by a 10 min incubation with 5 μM CsA (*lower trace*).

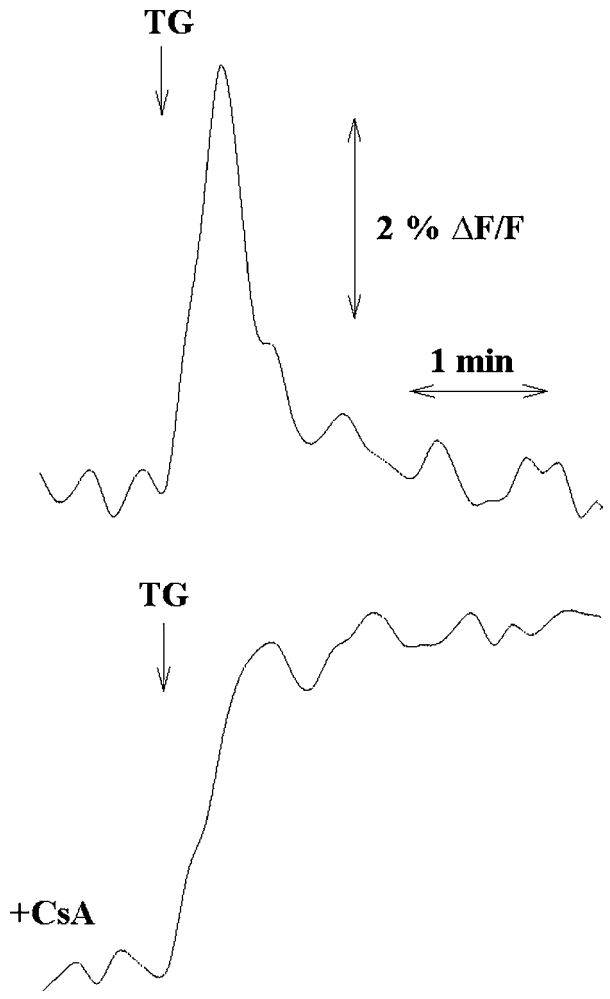

Fig. 9. Mitochondrial Ca^{2+} response when the SER pool was depleted by TG. Cells loaded with Rhod-2 in ECM with Ca^{2+} were diluted at 25°C in ECM with EGTA to give ~ 3×10^5 cells/mL in a nominally Ca^{2+}-free medium. The time-dependent response when 3 μM TG was added to the medium is shown (*upper trace*). The TG addition was preceded by a 10 min incubation with 5 μM CsA (*lower trace*).

DISCUSSION

Fluo-3 exhibited low fluorescence when loaded into nonstimulated H9c2 cells and high fluorescence, that was more intense in the nucleus, after addition of the Ca^{2+} ionophore IO (Fig. 1(A) and (B)). Higher nuclear fluorescence using Fluo-3 has already been reported in several cell types (Perez-Terzic *et al.*, 1997). However, it has been suggested that the difference in fluorescence intensity may be the result of distinct dye characteristics in different cellular compartments. Whatever the reason, the fluorescence intensity obtained from a cell suspension loaded with Fluo-3 faithfully reproduces the cytoplasmic Ca^{2+} response. This occurs when transient Ca^{2+} signals are generated in the cytoplasm and the nuclear region appears highly fluorescent (Gee *et al.*, 2000). The fluorescence pattern was clearly different when cells were loaded with dihydroRhod-2 (Fig. 1(C)) or TMRM (Fig. 1(D)). As previously published, bright tiny spots were observed in the cytoplasmic region when cells were loaded with the mitochondrial probes, whereas the nuclei were practically nonfluorescent. In our spectrofluorometric assays, the preliminary reduction of Rhod-2 was essential for obtaining a selective mitochondrial Ca^{2+} signal. The use of Rhod-2

without reduction resulted in a mainly cytoplasmic Ca^{2+} response.

Ca^{2+} mobilized by VP gave rise to a transient increase in cytoplasmic Ca^{2+} followed by a fall to the initial resting level (Fig. 2). The VP-induced Ca^{2+} peak was exactly the same whether cells were resuspended in ECM with Ca^{2+} or diluted in ECM with Ca^{2+} plus 10 mM Ni^{2+} (data not shown). Interestingly, the resting level following the Ca^{2+} peak was dependent on the ECM composition when the Ca^{2+}-mobilizing agent was TG (Fig. 3). The cytoplasmic level remained high after the Ca^{2+} peak when ECM with Ca^{2+} was used and this can be attributed to the capacitative Ca^{2+} entry. The time-course of net Ca^{2+} influx driven by the capacitative entry and partially counteracted by extrusion mechanisms can be derived as shown in Fig. 3B. However, cytoplasmic Ca^{2+} returned to the initial resting level when ECM with Ca^{2+} was supplemented with excess Ni^{2+} since Ca^{2+} entry from the extracellular space was prevented by the Ca^{2+}-channel blocker Ni^{2+} (Soboloff and Berger, 2002). It seems that Ca^{2+} extrusion mechanisms are relevant for maintaining the physiological resting level when the SER pool is unable to store Ca^{2+}, as long as Ca^{2+} entry from the external space is impeded. Ca^{2+} extrusion mechanisms do not play a significant role when the cytoplasmic Ca^{2+} signal is generated by VP. In this case, the resting Ca^{2+} level is recovered by the potent uptake mechanism associated with the SER Ca^{2+}-ATPase protein.

The cytoplasmic Ca^{2+} response to TG is critically dependent on the concentration ratio between TG and cells. Therefore, it is important to establish effective concentrations under specific assay conditions. In fact, variations in the effective concentration reported in the literature can be attributed to different experimental variables. Thus, the cytoplasmic Ca^{2+} response to nM TG (Fig. 4(A)) can be attributed to a direct effect on the SER Ca^{2+} pool. However, the use of higher TG concentrations triggers a more complex Ca^{2+} signal (data not shown). The SR Ca^{2+} pool responded to BHQ with a lower affinity than TG (Fig. 4(B)) but was insensitive to ryanodine. The absence of a Ca^{2+} response to ryanodine was consistent with the lack of a caffeine effect and the absence of ryanodine receptor in H9c2 myoblasts, but not in differentiated myotubes (Szalai *et al*., 2000).

A $\Delta\Psi_m$ value of *ca*. −200 mV is maintained by an electrical potential difference and a pH gradient. Thus, agents that decreased $\Delta\Psi_m$, such as the H^+ gradient-dissipating agent CCCP, released Ca^{2+} from the mitochondria (Fig. 5). However, the addition of the Ca^{2+} ionophore IO had a very limited decreasing effect on $\Delta\Psi_m$ (Fig. 7) and did not abolish the CCCP-induced Ca^{2+} release (Fig. 6). This indicates that the mitochondrial Ca^{2+} pool was maintained by $\Delta\Psi_m$ which was negative inside the organelle. Likewise, a SER Ca^{2+} signal such as that induced by TG was reflected as a small and transient depolarization of the inner mitochondrial membrance (Fig. 7).

Taking into consideration the effect of Ca^{2+}-mobilizing agents on cytoplasmic Ca^{2+} measured either in ECM with EGTA or in ECM with Ca^{2+} plus Ni^{2+}, it is confirmed that SER and mitochondria are major intracellular Ca^{2+} pools (Fig. 6). Moreover, excess IO produced complete discharge of the SER pool when cells were in a Ca^{2+}-free medium but had little effect on the mitochondrial store (Fig. 6). Also, the observed Ca^{2+} release induced by IO when added to cells in a Ca^{2+}-free medium after TG and CCCP was probably due to incomplete discharge of the above mentioned Ca^{2+} pools and/or the existence of an additional Ca^{2+} pool related with the Golgi apparatus. The presence of a Ca^{2+} pool and the expression of TG-insensitive Ca^{2+}-ATPase in the Golgi apparatus have been described (Missiaen *et al*., 2001; Pinton *et al*., 1998).

The presence of 1 mM Ca^{2+} in ECM guarantees that intracellular Ca^{2+} stores maintain a physiological Ca^{2+} load. However, Ca^{2+} responses from intracellular sources may be confused with Ca^{2+} entry from the external space. When the external medium was ECM with EGTA, to prevent entry of extracellular Ca^{2+}, there was a slow time-dependent depletion of intracellular stores. In fact, the resting Ca^{2+} level of cells diluted in ECM with EGTA was lower than in cells resuspended in ECM with Ca^{2+} (45 *vs*. 80 nM). Therefore, ECM with EGTA allows a qualitative estimation of intracellular Ca^{2+} pools. The best option for analyzing intracellular Ca^{2+} pools is ECM with Ca^{2+} plus excess Ni^{2+}. This latter medium prevents the partial depletion of intracellular stores and avoids the entry of external Ca^{2+} (Fig. 6).

The SER/mitochondria interplay has been shown to act as a physiological mechanism in Ca^{2+} signaling (Csordás and Hajóczky, 2003; Hajnóczky *et al*., 1995; Szalai *et al*., 2000). Thus, the Ca^{2+} signal transmission from SER to mitochondria in HeLa and other cell models was more effective when mediated by IP_3 than by other alternative mechanisms (Rizzuto *et al*., 1994). Moreover, studies on isolated hepatocytes demonstrate that mitochondria are able to discriminate fast and large-amplitude Ca^{2+} signals mediated by IP_3 from slow and smaller Ca^{2+} signals (Hajnóczky *et al*., 1995). Other studies on HeLa cells indicate that the cytoplasmic Ca^{2+} signals generated by different mechanisms and showing different spatiotemporal characteristics can be sensed by the mitochondria (Collins *et al*., 2001).

The cytoplasmic Ca^{2+} peak induced by VP in H9c2 cells evoked a transient Ca^{2+} signal in the mitochondria (Fig. 8), which was not perturbed by preincubation with CsA. Therefore, Ca^{2+} exit from the mitochondria subsequent to a reversible discharge of the SER Ca^{2+} pool, i.e., a physiological Ca^{2+} response, does not occur through the permeability transition pore.

When the cytoplasmic Ca^{2+} signal was generated by TG, the mitochondrial effect was also manifested as a Ca^{2+} peak (Fig. 9). However, the mitochondrial Ca^{2+} release induced by the irreversible discharge of the SER Ca^{2+} pool, i.e., a nonphysiological response, involves the permeability transition pore. The opening of the permeability transition pore and the loss of mitochondrial function are well established events linked to apoptotic death of the cell (Orrenius *et al*., 2002).

A detailed characterization of Ca^{2+} handling in our cell model and the links between intracellular Ca^{2+} pools is essential for further studies on Ca^{2+} signals that can be generated under physiological or pathological conditions.

ACKNOWLEDGMENTS

This study was supported by grants BMC2002-02474 from the Spanish Ministerio de Ciencia y Tecnología/Fondo Europeo de Desarrollo Regional and PI-22/00756/FS/01 from Fundación Séneca de la Comunidad Autónoma de Murcia, Spain. We express our appreciation to Dr. García-Estan and Dr. Marín Atucha from the School of Medicine Department of Physiology for the use of the Aminco-Bowman spectrofluorometer.

REFERENCES

Allen, D. G., and Blinks, J. R. (1978). *Nature* **273**, 509–513.
Altschuld, R. A., Hohl, C. M., Castillo, L. C., Garleb, A. A., Starling, R. C., and Brierley, G. P. (1992). *Am. J. Physiol.* **262**, H1699–H1704.
Babcock, D. F., Herrington, J., Goodwin, P. C., Park, Y. B., and Hille, B. (1997). *J. Cell Biol.* **136**, 833–844.
Berridge, M. J. (2002). *Cell Calcium* **32**, 235–249.
Berridge, M. J. (2003). *Biochem. Soc. Trans.* **31**, 930–933.
Berridge, M. J., Bootman, M. D., and Roderick, H. L. (2003). *Nat. Rev. Mol. Cell Biol.* **4**, 517–529.
Blinks, J. R., Wier, W. G., Hess, P., and Prendergast, F. (1982). *Prog. Biophys. Mol. Biol.* **40**, 1–114.
Bootman, M. D., Lipp, P., and Berridge, M. J. (2001). *J. Cell Sci.* **114**, 2213–2222.
Bowser, D. N., Minamikawa, T., Nagley, P., and Williams, D. A. (1998). *Biophys. J.* **75**, 2004–2014.
Broekemeier, K. M., Dempsey, M. E., and Pfeiffer, D. R. (1989). *J. Biol. Chem.* **264**, 7826–7830.
Chen, W.-C., and Chen, C.-C. (1999). *Endocrinology* **140**, 1639–1648.
Cheng, H., Lederer, W. J., and Cannell, M. B. (1993). *Science* **262**, 740–744.
Clapham, D. E. (1995). *Cell* **80**, 259–268.
Collins, T. J., Lipp, P., Berridge, M. J., and Bootman, M. D. (2001). *J. Biol. Chem.* **276**, 26411–26420.
Csordás, G., and Hajóczky, G. (2003). *J. Biol. Chem.* **278**, 42273–42282.
Duchen, M. R. (2000). *J. Physiol.* **529**, 57–68.
Fabiato, A. (1988). *Methods Enzymol.* **157**, 378–417.
Gee, K. R., Brown, K. A., Chen, W.-N.U., Bishop-Stewart, J., Gray, D., and Johnson, I. (2000). *Cell Calcium* **27**, 97–106.
Grynkiewicz, G., Poenie, M., and Tsien, R. Y. (1985). *J. Biol. Chem.* **260**, 3440–3450.
Hajnóczky, G., Csordás, G., Madesh, M., and Pacher, P. (2000). *J. Physiol.* **529**, 69–81.
Hajnóczky, G., Robb-Gaspers, L. D., Seitz, M. B., and Thomas, A. P. (1995). *Cell* **82**, 415–424.
He, H., Li, H. L., Lin, A., and Gottlieb, R. A. (1999). *Cell Death Differ.* **6**, 987–991.
Kass, G. E. N., Duddy, S. K., Moore, G. A., and Orrenius, S. (1989). *J. Biol. Chem.* **264**, 15192–15198.
Koizumi, S., Bootman, M. D., Bobanovic, L. K., Schell, M. J., Berridge, M. J., and Lipp, P. (1999). *Neuron* **22**, 125–137.
Lytton, J., Westlin, M., and Hanley, M. R. (1991). *J. Biol. Chem.* **266**, 17067–17071.
Mestril, R., Chi, S. H., Sayen, M. R., and Dillmann, W. H. (1994). *Biochem. J.* **298**, 561–569.
Missiaen, L., Van Acker, K., Parys, J. B., De Smedt, H., Van Baelen, K., Weidema, A. F., Vanoevelen, J., Raeymaekers, L., Renders, J., Callewaert, G., Rissuto, R., and Wuytack, F. (2001). *J. Biol. Chem.* **276**, 39161–39170.
Mizukami, Y., Kobayashi, S., Uberall, F., Hellbert, K., Kobayashi, N., and Yoshida, K. (2000). *J. Biol. Chem.* **275**, 19921–19927.
Monteith, G. R., and Blaustein, M. P. (1999). *Am. J. Physiol.* **276**, C1193–C1204.
Orrenius, S., Zhivotovsky, B., and Nicotera, P. (2002). *Nat. Rev. Mol. Cell Biol.* **4**, 552–565.
Perez-Terzic, C., Stehno-Bittel, L., and Clapham, D. E. (1997). *Cell Calcium* **21**, 275–282.
Pinton, P., Pozzan, T., and Rizzuto, R. (1998). *EMBO J.* **17**, 5298–5308.
Rizzuto, R., Bastianutto, C., Brini, M., Murgia, M., and Pozzan, T. (1994). *J. Cell Biol.* **126**, 1183–1194.
Rudolf, R., Morguillo, M., Rizzuto, R., and Pozzan, T. (2003). *Nat. Rev. Mol. Cell Biol.* **4**, 579–586.
Sagara, Y., and Inesi, G. (1991). *J. Biol. Chem.* **266**, 13503–13506.
Scaduto, R. C., and Grotyohann, L. W. (1999). *Biophys. J.* **76**, 469–477.
Schwartzenbach, G., Senn, H., and Anderegg, G. (1957). *Helv. Chim. Acta* **40**, 1886–1900.
Soboloff, J., and Berger, S. A. (2002). *J. Biol. Chem.* **277**, 13812–13820.
Szalai, G., Csordás, G., Hantash, B. M., Thomas, A. P., and Hajnóczky, G. (2000). *J. Biol. Chem.* **275**, 15305–15313.
Tanno, M., Bassi, R., Gorog, D. A., Saurin, A. T., Jiang, J., Heads, R. J., Martin, J. L., Davis, R. J., Flavell, R. A., and Marber, M. S. (2003). *Circ. Res.* **93**, 254–261.
Thomas, A. P., Alexander, J., and Williamson, J. R. (1984). *J. Biol. Chem.* **259**, 5574–5584.
Thomas, D., Lipp, P., Tovey, S. C., Berridge, M. J., Li, W. H., Tsien, R. Y., and Bootman, M. D. (2000). *Curr. Biol.* **10**, 8–15.
Woods, N. M., Cuthbertson, K. S. R., and Cobbold, P. H. (1986). *Nature* **319**, 600–602.
Yue, D. T., Marban, E., and Wier, W. G. (1986). *J. Gen. Physiol.* **87**, 223–242.